doi:10.3788/gzxb20184703.0306006

基于 Terfenol-D 材料和光纤光栅法布里珀罗腔的磁场传感器

马瑞[1,2],张文涛[1,2],王兆刚[1,2],黄稳柱[1,2],李芳[1,2]
(1 中国科学院半导体研究所 传感技术国家重点实验室,北京 100083)
(2 中国科学院大学 材料科学与光电技术学院,北京 100049)

摘 要:基于 Terfenol-D 磁致伸缩材料和光纤光栅法布里珀罗腔,提出了一种用于微弱静态磁场测量的光纤磁场传感器.为了提高传感器的分辨率,采用钕铁硼永磁体提供偏置磁场,同时,采用 Monel-400 合金与光纤光栅法布里珀罗腔耦合的方式,作为参考元件,对传感器进行温度补偿.实验测得传感器的磁场灵敏度为 1.7×10^{-3} pm/μT,磁场分辨率为 3.0 μT。实验结果表明,本传感器对于静态磁场响应具有良好的线性度和指向性,可用于微弱磁场测量.

关键词:光纤传感器;光纤布喇格光栅;光纤光栅法布里珀罗腔;磁致伸缩材料;磁场;温度
中图分类号:TP212 **文献标识码**:A **文章编号**:1004-4213(2018)03-0306006-7

Magnetic Sensor Based on Terfenol-D Materials and Fiber Bragg Grating Fabry-Perot Cavity

MA Rui[1,2], ZHANG Wen-tao[1,2], WANG Zhao-gang[1,2], HUANG Wen-zhu[1,2], LI Fang[1,2]
(1 *State Key Laboratory of Transducer Technology, Institute of Semiconductors, Chinese Academy of Sciences, Beijing* 100083, *China*)
(2 *College of Materials Science and Opto-Electronic Technology, University of Chinese Academy of Sciences, Beijing* 100049, *China*)

Abstract: A fiber optic magnetic sensor for the measurement of weak static magnetic field, based on Terfenol-D materials and Fiber Bragg Grating Fabry-Perot (FBG-FP) cavity, is proposed and demonstrated. In order to improve the sensitivity of the sensor, a NdFeB magnet is used to apply bias magnetic field. To compensate the environmental temperature, another FBG-FP coupled with Monel-400 is used as a reference. The measurement sensitivity of the sensor is 1.7×10^{-3} pm/μT, which results in a magnetic induction resolution of 3.0 μT. The experimental results show that the sensor exhibits excellent linearity and directivity in response to static magnetic field.

Key words: Fiber optic sensors; Fiber Bragg grating; Fiber Bragg grating Fabry-Perot cavity; Magnetostrictive material; Magnetic field; Temperature
OCIS Codes: 060.2300; 060.2310; 060.2370; 060.3735; 280.4788

Foundation item: The Youth Innovation Promotion Association of CAS (No. 2016106), and Key R&D Program of China (No. 2017YFB0405503)

First author: MA Rui (1993—), male, M.S. degree candidate, mainly focuses on fiber grating sensing technology. Email: marui@semi.ac.cn
Supervisor(Corresponding author): ZHANG Wen-tao (1980—), male, professor, Ph.D. degree, mainly focuses on optical fiber sensing technology. Email: zhangwt@semi.ac.cn

Received: Sep.18, 2017; **Accepted**: Nov.22, 2017

0 Introduction

Fiber optic magnetic field sensors have attracted increasing attention because oftheir advantages such as anti-electromagnetic interference, light weight, small size and so on[1]. Moreover, fiber optic magnetic field sensors can be used for a wide range of applications, such as biomedical fields, hazard forecast, current measurement[2-3]. Based on different measurement principles, fiber optic magnetic sensors can be classified into several types. According to Faraday effect, fiber optic sensors can detect magnetic field directly by measuring the Faraday rotation angle of the light polarization[4]. Another type of fiber magnetic sensors is based on Ampere′s force[5]. The disadvantage of this kind of sensors is the essential of stimulation current. In addition, fiber magnetic sensors using Magnetic Fluid (MF) as cladding or filling MF into photonic crystal fiber are hotspots in recent years[6-7]. Fiber optic magnetic field sensors with magnetostrictive materials have been proposed for decades[8]. The fundamental principle of this type of sensors is that the longitudinal strain of magnetostrictive materials induced by magnetic fields can be transferred to fiber optic strain sensors, which can be based on a Michelson interferometer[9], Fabry-Perot interferometer[10], fiber-grating laser[11], phase-shifted fiber Bragg grating[12], fiber Bragg gratings[13], long period gratings[14]. Among all the magnetostrictive materials, Terfenol-D ($Tb_{0.3}Dy_{0.7}Fe_{1.92}$) has become the most frequently used giant magnetostrictive material because of its large magnetostrictive coefficient, high reliability, fast response speed, wide temperature range and so on[15].

For magnetic field sensors based on Terfenol-D and FBG, the magnetostriction of Terfenol-D leads to the Bragg wavelength shift of FBG. The reflection spectrum bandwidth of FBG is critical to the wavelength resolution. Compared to FBG, the reflect spectrum bandwidth of Fiber Bragg Grating Fabry-Perot (FBG-FP) cavity is much narrower[16]. In this manuscript, we propose a special sensor design using a FBG-FP bonded with Terfenol-D to achieve higher static resolution of magnetic field.

1 Structure model

The proposed fiber optic magnetic sensor is shown in Fig.1. The Terfenol-D rod, in a size of Φ5 mm×35 mm, is fixed in the frame. The two supports are fixed at both ends of the Terfenol-D rod. FBG-FP is installed between the two supports, using epoxy resin. To avoid bending, a pre-strain is applied on the FBG-FP during the assembling process. The NdFeB magnet is a kind of permanent magnet, which is in a size of Φ8 mm×3 mm. The magnetic field intensity on its surface is 50 mT. The NdFeB magnet will apply a bias magnetic field along with the Terfenol-D rod, which means the Terfenol-D rod will further elongate when a positive magnetic field is applied and will contract when a negative magnetic field is applied. The spring is fixed between the NdFeB magnet and the frame. It will be compressed when the Terfenol-D rod elongates. To eliminate the effect of the magnetic field, all the components are made of non-magnetic aluminum except the NdFeB magnet and the Terfenol-D rod.

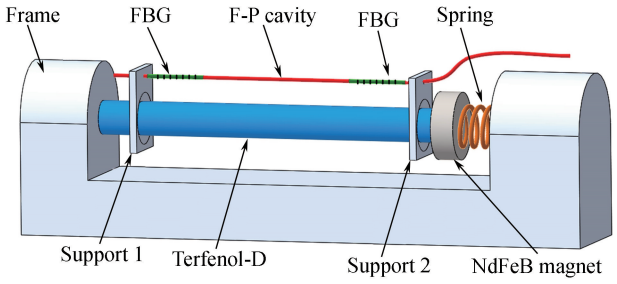

Fig.1 Schematic of the fiber magnetic field sensor

FBG-FP used in the sensor is formed by writing two identical FBGs 14 mm distant in a single mode fiber. The parameters of the FBG-FP as: nominal Bragg wavelength is 1 549.650 nm, bandwidth is 0.22 nm and peak reflectivity is 99.5%. The Free Spectral Range (FSR) and the bandwidth of the FBG-FPs are 60 pm and 0.9 MHz, respectively.

2 Sensing principle

The Terfenol-D rod will exhibit longitudinal extension when the external magnetic field or the temperature changes. The relationship between the strain of Terfenol-D rod ε_T and the external magnetic field H is given by

$$\varepsilon_T = \frac{\Delta L}{L} = C_f H^2 \tag{1}$$

where ΔL is the change in length imposed by Terfenol-D, L is the length of Terfenol-D rod, C_f is the magnetostrictive coefficient.

The twosupports will move with the change of the rod length simultaneously. The deformation will lead to wavelength shift of FBG-FP as

$$\Delta\lambda_1 = [(1-p_e)\varepsilon_0 + \alpha_1 T]\lambda_c \tag{2}$$

where p_e is the effective elastic-optic coefficient of the fiber, which is 0.22, ε_0 is the strain of the FBG-FP, α_1 is the thermal expansion coefficient of Terfenol-D, λ_c is the peak wavelength of FBG-FP, which is 1 549.650 nm.

To compensate the temperature effect, another FBG-FP fixed on a Monel-400 rod is used as a reference. Monel-400 is a kind of non-magnetic alloys which has similar thermal expansion coefficient with Terfenol-D. The relationship of the peak wavelength shiftof FBG-FP and temperature can be expressed as

$$\Delta\lambda_2 = \alpha_2 T\lambda_c \tag{3}$$

where α_2 is the thermal expansion coefficient of Monel-400. The thermal expansion coefficient between Terfenol-D and Monel-400 is similar, so $\alpha_1 = \alpha_2 = \alpha$. Subtracting Eq. (3) from Eq. (2), we get

$$\Delta\lambda = (1-p_e)\varepsilon_0\lambda_c \tag{4}$$

Ideally, $\varepsilon_0 = \varepsilon_T = \varepsilon$. We can obtain the relationship between the shift in the peak wavelength of FBG-FP and the external magnetic field

$$\Delta\lambda = C_f(1-p_e)\lambda_c H^2 \tag{5}$$

Thus, the sensitivity of this sensor can be expressed as

$$S_H = \frac{d\Delta\lambda}{dH} = 2C_f(1-p_e)\lambda_c H \tag{6}$$

The Terfenol-D rod will reach its maximum value of $1\times10^{-3}\,\varepsilon$ when the magnetic field is over 100 mT (provided by Huizhou South Rare Earth Functional Material Institute Co.). In a weak magnetic field, we suppose that the strain of Terfenol-D rod is proportional to the magnetic field. According to Eq. (4), we assume that the wavelength variation of FBG-FP is proportional to the magnetic field. And we have already known that the effective elastic-optic coefficient is 0.22 and the peak wavelength of FBG-FP is 1 549.650 nm. Hence, the approximate theoretical magnetic field sensitivity of the sensor is calculated to be 1.2×10^{-2} pm/μT. Additionally, according to Eq. (6), when a bias magnet is applied, the sensitivity of the sensor will be increased significantly.

3 Experimental setup

In order to detect the wavelength shift, the schematic of the demodulation system is proposed as is shown in Fig. 2. The beam from the tunable fiber laser (NKT Laser E15, wavelength range is 1 535-1 580 nm, maximum output power is 40 mW, linewidth is 100 Hz) is spilt into a pair of FBG-FPs, which is used as the sensing element and the referencing element, respectively. The reflection spectra of FBG-FPs are detected by photodiodes (KG-BPR-200 M, spectral response range is 850 nm-1 650 nm, 3 dB bandwidth is 200 M). The reflection spectra are processed by the cross-correlation method, and the strain of the sensing FBG-FP can be demodulated[16].

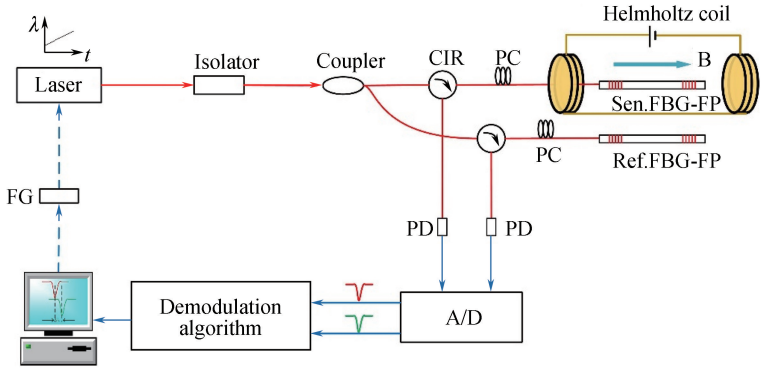

Fig.2 Schematic of the demodulation system

The measurement principle of this system is using the tunable fiber laser to scan FBG-FP. We can obtain $\Delta\lambda$ by calculating the wavelength difference of the peak positions of two FBG-FPs. The linear scanning range of the tunable fiber laser is 60 pm. In last chapter, the theoretical magnetic field sensitivity is calculated to be 1.2×10^{-2} pm/μT, which means that the magnetic field measurement range is -50 mT to 50 mT.

The experiment setup is shown in Fig.3. The magnetic shielding room is wrapped with two layers of high purity aluminum and eight layers of permalloy, which is used to shield the geomagnetic field. The residualmagnetic field in the magnetic shielding room is less than 20 nT. The Helmholtz coil is used to produce a uniform static magnetic field. The diameter of the coil is 60 cm, and the diameter of the uniform region is 40 cm. The high-precision constant current source is used to control the magnitude and direction of the current. It can provide a magnetic field from -100 μT to 100 μT. The magnetic field sensor is placed in the uniform region of the Helmholtz coil.

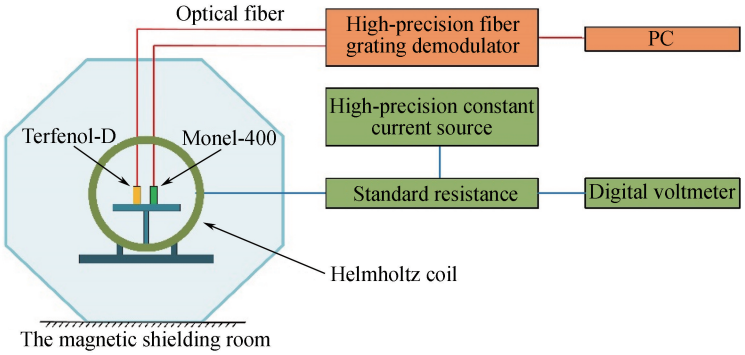

Fig.3 Schematic of the test system

4 Results and discussions

The effect of temperature compensation is tested before the measurement of magnetic field. We record the peak wavelength difference between two FBG-FPs in the absence of external magnetic field. Fig. 4 shows the result within 60 s. The measurement accuracy of this sensor is about 5×10^{-3} pm after temperature compensation in this environment. This value is five times lower than the previous measured value[16]. This is because the thermal expansion coefficient of Terfenol-D and Monel-400 is not exactly the same. Therefore, this method cannot fully compensate the effect of temperature.

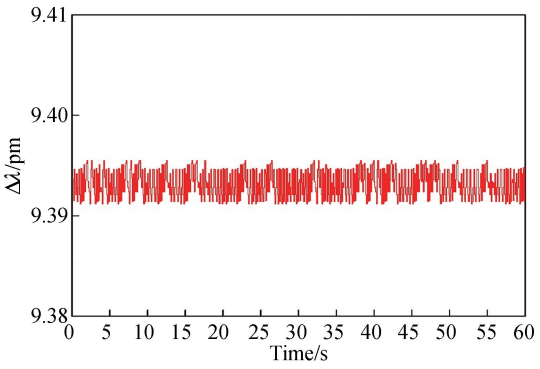

Fig.4 Peak wavelength difference within 60 s

In Fig. 5, the real-time response of the magnetic field sensor is observed and obtained with the demodulation system shown in Fig. 2. The static magnetic field is varied from -100 μT to 100 μT. The magnetic field increases by 50 μT every 30 s. As the result of the bias magnetic field provided by the permanent magnetic, response of the Terfenol-D to positive and negative magnetic fields is different. The Terfenol-D rod elongates or shortens when the direction of the external magnetic changes. In Fig.5, it is shown that the peak wavelength difference between two FBG-FPs changes immediately as the external magnetic field changes, which means that this sensor has fast response speed

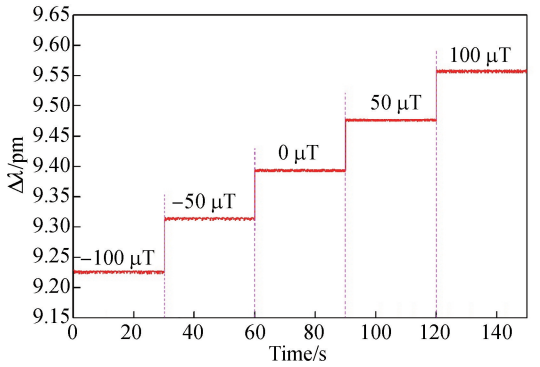

Fig.5 Sensor response to magnetic field changes

to the applied magnetic field.

In Fig. 6, we compare the response of this sensor to the external magnetic field with or without the permanent magnet. The peak wavelength difference between two FBG-FPs changes with the increase of static magnetic field from -100 μT to 100 μT. The step length is 10 μT. The sensitivity responses of the magnetic field sensor for non-magnetic bias and magnetic bias are 5.0×10^{-4} pm/μT and 1.7×10^{-3} pm/μT, respectively. It can be concluded that the sensitivity of sensor under magnetic bias is about 3.4 times higher than the sensitivity of sensor without magnetic bias. A standard deviation error in each step is present, but they are too small to be observed in the plot.

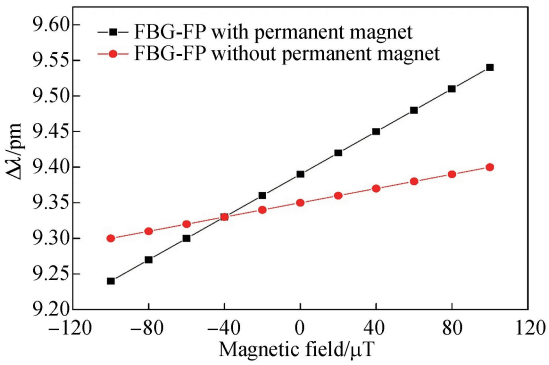

Fig.6 Schematic of the fiber magnetic field sensor

According to Eq. (6), the sensitivity of this sensor is related to the value of magnetic field. Thus, the slope of the curve will increase if a bias magnetic field is applied. As is said before, the measurement accuracy of this sensor is about 5×10^{-3} pm, so, it can be calculated that this magnetic field senor with magnetic bias has a resolution of 3.0 μT. It is also the detection limit of this sensor.

The measured sensitivity is lower than the theoretical sensitivity. That's probably because of the bonding between fiber and Terfenol-D rod. The strain of the Terfenol-D rod can't lead to the peak wavelength shift of FBG-FP completely. In addition, the theoretical calculation of the sensitivity of sensor is simplified. According to Eq. (6), the sensitivity of sensor is related to the value of magnetic field. Therefore, the sensitivity will be lower than expected when the external magnetic is weak.

Because of the narrow-bandwidth notch of the reflection spectrum of FBG-FP, the resolution of this sensor are much higher than sensors based on Phase-Shifted Fiber Bragg Grating (PS-FBG)[12], FBG[13], Long Period Gratings (LPG)[14]. Additionally, the resolution can be further improved in several ways, such as ameliorating the temperature compensate effect, enhancing the magnetic field intensity of the permanent magnet, narrowing the bandwidth of the spectrum notch of FBG-FP.

Table 1 Magnetic field sensitivity and resolution of different methods

Methods	FBG-FP	PS-FBG[12]	FBG[13]	LPG[14]
Resolution /μT	3	23	60	200

Directivity is also important to magnetic sensors. In order to test the directivity of the sensor more precisely, we remove the NdFeB magnet of the sensor. The relationship between the response of the sensor and each rotation angle can be expressed as

$$\Delta\lambda_\theta = \Delta\lambda_{\max} \cdot \cos\theta \tag{7}$$

where $\Delta\lambda_\theta$ is the peak wavelength difference between two FBG-FPs due to the exteral magnetic field, $\Delta\lambda_{\max}$ is the peak wavelength difference between two FBG-FPs if the external magnetic field is parallel to the Terfenol-D rod, and θ is the angle between the exteral magnetic field and the axial direction of the Terfenol-D rod.

As is shown in Fig.7, the directivity test can be implemented by putting the senor on a rotating stage at the center of Helmholtz coil and rotating it at various angles. The magnitude of magnetic field is set to 100 μT. The magnetic field is applied on the sensor with rotating the sensor from 0° to 360° in a step of 10°.

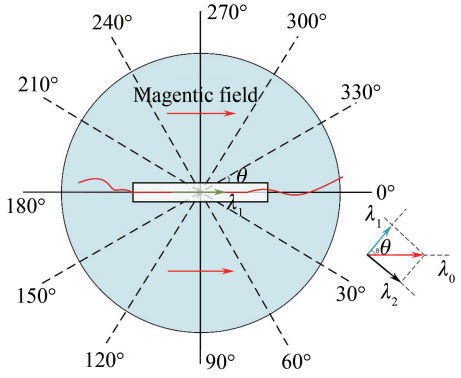

Fig.7 Measurement of the directivity of the sensor

Fig.8 shows the variation of the responsivity at different angles. 0 dB means the sensor reaches its maximum sensitivity when the Terfenol-D rod is parallel to the direction of the magnetic field. The sensor exhibits its minimum response when the Terfenol-D rod and the external magnetic field are vertical. As is shown in Fig.8, the measured value matches well with the theoretical value, which is drawn from Eq. (7). The imperfect symmetry exists, which may result from the hysteresis effect of Terfenol-D material. Hysteresis effect will make the elongation of the Terfenol-D rod vary even in the symmetrical direction. In addition, the errors of the rotating stage cannot be ignored.

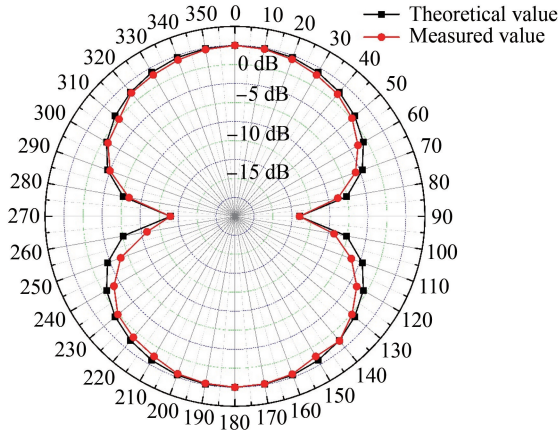

Fig.8 Variation of the peak wavelength difference between two FBG-FPs

5 Conclusion

In conclusion, a compact fiber optic sensor based on FBG-FP andTerfenol-D is proposed and demonstrated for weak static magnetic field detection. It is proved that the method of temperature compensation is effective and can be more efficient by choosing material which has the same thermal expansion coefficient with Terfenol-D. The real-time response of sensor shows that it has fast response speed. A permanent magnet is used to apply magnetic bias and the sensitivity of sensor with magnetic bias is about 3.4 times higher than the sensitivity without magnetic bias. As a result of the extremely narrow notch of FBG-FP, the sensor exhibits a sensitivity of 1.7×10^{-3} pm/μT. The resolution of this sensor is 3 μT, which is much higher than sensors based on PS-FBG, FBG, LPG. In addition, the sensitivity and resolution of sensor can be improved by using another bias magnet which has a larger magnetic field. This sensor also presents orientation-dependence of magnetostriction, which has a potential to be fabricated as a tri-axial sensor.

References

[1] DESIMONE A, JAMES R D. A theory of magnetostriction oriented towards applications[J]. *Journal of Applied Physics*, 1997, **881**(8): 5706-5708.

[2] DENG Ming, LIU Dan-hui, HUANG Wei, *et al*. Highly-sensitive magnetic field sensor based on fiber ring laser[J]. *Optics Express*, 2016, **24**(1): 645-651.

[3] SHEN Tao, FENG Yue, SUN Bin-chao, *et al*. Magnetic field sensor using the fiber loop ring-down technique and an etched fiber coated with magnetic fluid[J]. *Applied Optics*, 2016, **55**(4): 673-678.

[4] CHENG Ling-hao, HAN Jian-lei, JIN Long, *et al*. Sensitivity enhancement of Faraday effect based heterodyning fiber laser magnetic field sensor by lowering linear birefringence[J]. *Optics Express*, 2013, **21**(25): 30156-30162.

[5] WANG Zhao-gang, ZHANG Wen-tao, HUANG Wen-zhu, *et al*. A fiber optic accelerometer-magnetometer[J]. *Journal of Lightwave Technology*, 2017, **35**(9):1732-1737.

[6] LUO Long-feng, PU Sheng-li, TANG Jia-li, *et al*. Reflective all-fiber magnetic field sensor based on microfiber and magnetic fluid[J]. *Optics Express*, 2015, **23**(14): 18133-18142.

[7] CHEN Yao-fei, HAN Qun, YAN Wen-chuan, *et al*. Magnetic-fluid-coated photonic crystal fiber and FBG for magnetic field and temperature sensing[J]. *IEEE Photonics Technology Letters*, 2016, **28**(23): 2665-2668.

[8] YARIV A, WINSOR H V. Proposal for detection of magnetic fields through magnetostrictive perturbation of optical fibers[J]. *Optics Letters*, 1980, **5**(3): 87-89.

[9] CHEN Fei-fei, JIANG Yi. Fiber optic magnetic field sensor based on the TbDyFe rod[J]. *Measurement Science & Technology*, 2014, **25**(8): 085106.

[10] ZHOU Bin, LU Chang-tao, BAREREMM M, *et al*. "Magnetic field sensor of enhanced sensitivity and temperature self-calibration based on silica fiber Fabry-Perot resonator with silicone cavity,"[J]. *Optics Express*, 2017, **25**(7): 8108-8114

[11] HE Wei, CHENG Ling-hao, YUAN Qiang, *et al*. Magnetostrictive composite material-based polarimetric heterodyning fiber-grating laser miniature magnetic field sensor[J]. *Chinese Optics Letters*, 2015, **13**(5): 17-20.

[12] SHAO Zhi-hua, QIAO Xue-guang, RONG Qiang-zhou, *et al*. Fiber-optic magnetic field sensor using a phase-shifted

fiber Bragg grating assisted by a TbDyFe bar[J]. *Sensors & Actuators A Physical*, 2017, **261**: 49-55.

[13] FILOGRANO M L, PISCO M, CATALANO A, *et al*. Triaxial fibre optic magnetic field sensor for magnetic resonance imaging[J]. *Journal of Lightwave Technology*, 2017, **35**(18): 3924-3933.

[14] GRAHAM C B L, TOM A, WANG Chang-le. Fiber optic sensing of magnetic fields utilizing femtosecond laser sculpted microslots and long period gratings coated with Terfenol-D[C]. 24th International Conference on Optical Fibre Sensors, 2015, **9634**: 1-4.

[15] ENGDAHL G. Handbook of GiantMagnetostrictive Materials[M]. Academic Press, 2000.

[16] HUANG Wen-zhu, ZHANG Wen-tao, ZHEN Teng-kun, *et al*. π-phase-shifted FBG for high-resolution static-strain measurement based on wavelet threshold denoising algorithm[J]. *Journal of Lightwave Technology*, 2014, **32**(22): 4294-4300.